Information Scrambling and Loschmidt Echo

Bin Yan,[1,2,3] Lukasz Cincio,[1] and Wojciech H. Zurek[1]
[1]*Theoretical Division, Los Alamos National Laboratory, Los Alamos, New Mexico 87545, USA*
[2]*Center for Nonlinear Studies, Los Alamos National Laboratory, Los Alamos, New Mexico 87545, USA*
[3]*Department of Physics and Astronomy, Purdue University, West Lafayette, Indiana 47907, USA*

(Received 18 March 2019; revised manuscript received 24 June 2019; accepted 31 March 2020; published 24 April 2020)

We demonstrate analytically and verify numerically that the out-of-time order correlator is given by the thermal average of Loschmidt echo signals. This provides a direct link between the out-of-time-order correlator—a recently suggested measure of information scrambling in quantum chaotic systems—and the Loschmidt echo, a well-appreciated familiar diagnostic that captures the dynamical aspect of chaotic behavior in the time domain, and is accessible to experimental studies.

DOI: 10.1103/PhysRevLett.124.160603

Introduction.—The study of the quantum version of classically chaotic systems gave rise to the field of quantum chaos, since it was realized that quantum chaotic systems share certain common characteristics [1,2]. In particular, in spite of the absence of the telltale exponential sensitivity to initial conditions in unitary quantum evolution, one can use as a quantum diagnostic of chaos sensitivity of the evolution to small perturbations of the Hamiltonian [3] or its entropy production in the presence of coupling to the environment [4,5]. These and related manifestations of quantum chaos have been by now widely studied [6–13], using diagnostics such as Loschmidt echo (LE) [14,15]:

$$M(t) \equiv |\langle\psi|e^{iH_0 t}e^{-i(H_0+V)t}|\psi\rangle|^2. \tag{1}$$

This quantity incorporates the simple idea [3] that small perturbations of the Hamiltonian may trigger dramatic changes of the dynamics, inducing the butterfly effect.

More recently, the out-of-time-order correlator (OTOC) [16,17], another diagnostic for quantum chaos, has been proposed and received considerable attention across many different fields in physics, including quantum information and high-energy and condensed matter physics [18–41]. The OTOC is defined as a four-point correlator with unusual time ordering:

$$F_\beta(t) \equiv \langle A^\dagger(t)B^\dagger A(t)B\rangle_\beta, \tag{2}$$

where A and B are typically chosen as local operators; $A(t) = e^{iHt}Ae^{-iHt}$ is the Heisenberg operator evolving under total Hamiltonian H and the average $\langle\rangle$ is taken over a thermal state at the inverse temperature β. In chaotic systems, the OTOC exhibits fast decay and converges to a persistent small value [17]. It was argued that, under certain natural assumptions, the exponential decay rate is bounded by $\lambda \le 2\pi/\beta$ [24,27]. Another benefit of the OTOC is that it is designed to probe the spreading of local information over the entire system. Moreover, for systems with spatial structures, information measured by the OTOC propagates ballistically with a finite velocity known as the butterfly velocity [23,37,38].

The OTOC is typically understood as an intrinsic echo-type quantity. For instance, when A and B are chosen as unitary operators, Eq. (2) can be directly measured by echo experiments [13,42–45]. There are efforts to build more direct links between these two quantities, e.g., using variants of the OTOC and LE or particular choices of operators for the OTOC evaluation [46–48]. However, the precise quantitative equivalence between the OTOC and the Loschmidt echo is still missing. Establishing such a relation would be beneficial for both areas and shed new light on the whole field of quantum chaos.

In this work, we accomplish the task of connecting the OTOC to the Loschmidt echo. We shall focus on the temporal decay of the OTOC without extra complications caused by spatial propagation. We demonstrate that the OTOC equals the thermal average of the Loschmidt echo. The coupling between the target local systems, i.e., the supports of the local operators, and the rest of the total system plays the role of a perturbation. To further support our theory, we present two model studies involving coupled inverted harmonic oscillators and a random matrix model.

Bridging the out-of-time-order correlator and Loschmidt echo.—For a chaotic Hamiltonian, the universal decay of the OTOC is insensitive to the form of operators A and B in Eq. (2), as long as they are generic, i.e., not reflecting the particular symmetries possessed by the Hamiltonian. Any generic choice of local operators, e.g., random operators, is representative for the universal decay of the OTOC. This allows us to look at the typical behavior of the OTOC by averaging all unitary operators on subsystem S_A and S_B:

$$\overline{F_\beta(t)} \equiv \int dAdBF_\beta(t), \tag{3}$$

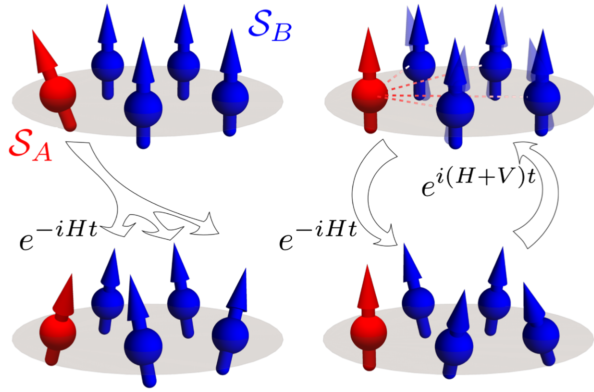

FIG. 1. An illustration of the system structure under consideration. S_A is a small local subsystem. S_B is chosen as the complement of S_A. (Left) A local perturbation on subsystem S_A spreads over the entire system during time evolution. This can be captured by the decay of OTOC in Eq. (2). (Right) The large subsystem S_B feels an effective random stochastic perturbation V induced by the interaction with the small subsystem S_A. Due to this effective perturbation, the dynamics of S_B becomes irreversible. This can be detected by the Loschmidt echo signal in Eq. (1). These two processes are shown to be related through the OTOC-LE correspondence in Eq. (9). Since S_A is small and local, one can effectively treat S_B as the total system.

where the integration is performed with respect to the Haar measure for unitary operators. Similar ideas have been considered in the literature [49–52]. Here, we will assume that A and B are supported on distinct local subsystems. For global operators, the OTOC has been shown to be closely related to the spectral form factor of the Hamiltonian [50,51,53]. As will be seen in the following, taking into account the local structure of the system is crucial to reveal the correct behavior of the OTOC.

For simplicity, we focus on the OTOC at an infinite temperature ($\beta = 0$). It is straightforward to generalize to a finite temperature by distributing the thermal density operator over a thermal loop, e.g., using the scheme described in Refs. [24,27,50]. The finite-temperature correction will be taken into account when discussing the temperature dependence of the decay rate.

We focus on the scenario that A is an operator with support on a small local subsystem S_A, while operator B is chosen such that its support S_B is the complement of S_A, as illustrated in Fig. 1. It is reasonable to expect that choosing operator B in such a manner also captures the spreading of operator A over the entire system, detected by its nonzero projection at later times on the support of operator B, at least in the bulk of the decay. Analysis of this particular scenario is also instructive and can be generalized in a similar way to cases where B is a small local operator as well.

The Haar integral over subsystem operators can be evaluated with the aid of the formula

$$\int dA A^\dagger O A = \frac{1}{d_A}\mathbb{I}_A \otimes \mathrm{tr}_A(O), \tag{4}$$

where $\mathbb{I}_A$ is the identity operator and tr_A is the partial trace over subsystem S_A. The Haar measure is unique up to a constant multiplicative factor. Here, d_A, the dimension of S_A, is introduced as a convention to normalize the OTOC [54]. The proof of the above equation is given in Appendix A of Supplemental Material [55].

The average over all random unitary operators on subsystem S_A gives us

$$\begin{aligned}\int dA F_{\beta=0}(t) &\equiv \frac{1}{d}\int dA \mathrm{tr}[A^\dagger(t)B^\dagger A(t)B] \\ &= \frac{1}{d}\frac{1}{d_A}\mathrm{tr}[\mathbb{I}_A \otimes \mathrm{tr}_A(e^{-iHt}B^\dagger e^{iHt})e^{-iHt}Be^{iHt}] \\ &= \frac{1}{d}\frac{1}{d_A}\mathrm{tr}_B[\mathrm{tr}_A(e^{-iHt}B^\dagger e^{iHt})\mathrm{tr}_A(e^{-iHt}Be^{iHt})].\end{aligned} \tag{5}$$

The last line of the above equation involves the reduced dynamics of operator B, i.e., $B(-t) \equiv \mathrm{tr}_A(e^{-iHt}Be^{iHt})$. In order to further perform the average over B, we estimate $B(-t)$ in the following way. The total system Hamiltonian, in general, has the structure

$$\begin{aligned} H &= \mathbb{I}_A \otimes H_B + H_A \otimes \mathbb{I}_B + H', \\ H' &\equiv \delta \sum_k V_A^k \otimes V_B^k. \end{aligned} \tag{6}$$

Here V_A^k's are Hermitian and orthonormal (with respect to the Hilbert-Schmidt inner product and norm); V_B^k's are Hermitian and orthogonal and have norms on the same order as H_B, such that δ quantifies the relative strength of the coupling. In realistic physical systems, the coupling parameter $\delta \ll 1$. To get the solution of $B(-t)$, we replace the effect of the coupling with an ensemble of random noises $\{V_\alpha\}$ on subsystem S_B, namely,

$$\begin{aligned} B(-t) &= \mathrm{tr}_A(e^{-iHt}Be^{iHt}) \\ &\propto \overline{e^{-i(H_B+V_\alpha)t}Be^{i(H_B+V_\alpha)t}}. \end{aligned} \tag{7}$$

Here α labels different realizations of the noise, and the average taken is over all realizations of the noise operator V_α's.

The above claim is based on the correspondence between the symptoms of decoherence [56,57] (process that involves entangling correlations between the system and the environment) and symptoms of the suitable external noises. In Appendix B of Supplemental Material [55], we back up this claim with a more mathematically rigorous treatment of the noise operators in terms of master equations up to the second order of the coupling parameter δ [58], where it is shown that the noise operators can be chosen as linear combinations of V_B^k's with random coefficients ± 1:

$$V_\alpha = \sum_k \pm \delta V_B^k. \tag{8}$$

With the aid of the alternative form for the reduced dynamics for $B(-t)$ in Eq. (7), averaging over operators B can be further performed in the same manner as for the operators A. This gives the final expression for the averaged OTOC:

$$\overline{F_{\beta=0}(t)} \approx \overline{|\langle e^{i(H_B+V_\alpha)t} e^{-i(H_B+V_{\alpha'})t}\rangle_{\beta=0}|^2}. \tag{9a}$$

Here, V_α and $V_{\alpha'}$ average over all realizations of the noise operators as given by Eq. (8). Each term in the average is precisely the Loschmidt echo averaged over a thermal ensemble. For systems with large number of degrees of freedom, the ensemble of noises is large, and the structures of the noise operators are expected to be not essential. In this case, one can replace the noise average with a single LE to get a coarse-grained version of the above equation, namely,

$$\overline{F_{\beta=0}(t)} \approx |\langle e^{i(H_B+V_1)t} e^{-i(H_B+V_2)t}\rangle_{\beta=0}|^2. \tag{9b}$$

Equation (9) is the main result of this work. Note that: (i) As has been mentioned before, the above result generalizes to finite temperatures. We present the full derivation in Appendix C of Supplemental Material [55], using the same scheme for regularizing the thermal state explored in Refs. [24,27,50]. This regularization scheme is crucial for the discussion of the bound of the OTOC decay [59]. (ii) The perturbations that appear in the LE emerge from the interactions nested in the total Hamiltonian. (iii) The OTOC has several decay regimes, e.g., the early growth $\sim a - \epsilon b e^{\lambda t} + O(\epsilon^2)$ before the scrambling (Ehrenfest) timescale [24], where a and b are order-1 numbers and $\epsilon \ll 1$ is a small parameter; or the intermediate pure exponential decay. The only approximation involved in the derivation of Eq. (9) is the second-order approximation of the coupling parameter δ. It will be shown in the following that the OTOC-LE connection holds in both the scrambling and intermediate decay regimes. Remarkably, the second order of the coupling parameter δ^2 is identified as the small prefactor ϵ in the early exponential growth, which determines the scrambling timescale $\sim(1/\lambda)\ln(1/\epsilon)$.

Case I: Early scrambling.—To verify the OTOC-LE relation in the scrambling regime, we first study an exactly solvable model consisting of two coupled inverted harmonic oscillators (IHOs), whose Hamiltonian is

$$\sum_{i=1,2}\left(\frac{1}{2m_i}\hat{p}_i^2 - \frac{m_i\omega_i^2}{2}\hat{x}_i^2\right) + \delta\hat{x}_1\hat{x}_2. \tag{10}$$

This model employs IHOs, as they were first used to emulate dynamical instability characteristic of quantum chaos in an exactly solvable system [60]. Their role here is

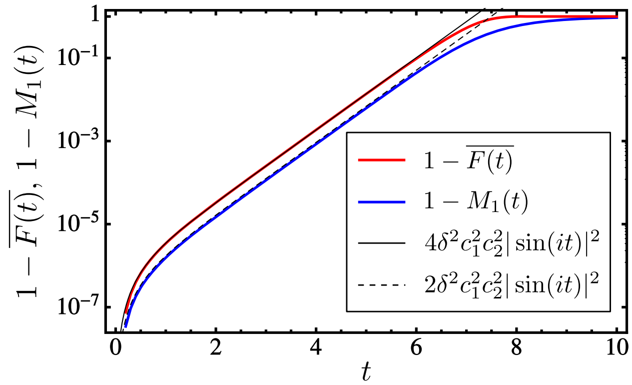

FIG. 2. Early exponential growth of the OTOC and LE of the IHOs. The average of the OTOC is taken over a pure product state $\psi(x_1)\psi(x_1) \propto e^{-x_1^2/m_2} e^{-x_2^2/m_1}$. The parameters are $m_1 = 10^5$, $m_2 = 1$, $\omega_1 = 0$, $\omega_2 = 1$, and $\delta = 10^{-5}$. The solid blue and red curves correspond to $1 - \overline{F(t)}$ and $1 - M_1(t)$, respectively. The dashed and solid black curves correspond to $2\delta^2 c_1^2 c_2^2|\sin(it)|^2$ and $4\delta^2 c_1^2 c_2^2|\sin(it)|^2$, respectively, as deduced from Eq. (12).

to capture the essential ingredients of the OTOC-LE relation: The OTOC is computed for two (local) operators on the two oscillators, respectively. The parameters are tuned as $m_1 \gg m_2$, $\omega_1 \ll \omega_2$, and $\delta \ll 1$ such that the dynamics of the first oscillator is much slower than the second one and the coupling is weak. Hence, oscillator 1 and 2 mimic the subsystems S_A and S_B, respectively.

Since the spectrum of the IHOs is not bounded from below, the thermal state is not well defined. We replace the regularized thermal state with a pure state $|\psi_1(x_1)\rangle|\psi_2(x_2)\rangle$. The pure state average of the OTOC has been considered in the literature [43]. In this case, the Haar averaged OTOC of the two coupled oscillators can be computed exactly. We depict the result in Fig. 2 and delegate the lengthy calculation to Supplemental Material [55], where it is shown that the pure state average carries out in the same manner as a thermal ensemble.

According to Eq. (9), the OTOC equals the LE of the second oscillator (the large subsystem S_B), which admits an exact solution as well. The perturbations emerging from the coupling are $\pm\delta c_1\hat{x}_2$ with equal probability, where $c_1^2 = \langle\psi_1|x_1^2|\psi_1\rangle$. Note that the average of x_1^2 appears because of the normalization condition in the decomposition of the interaction in Eq. (6). See details about the derivation of the perturbation operators in Ref. [55]. As a simple system, the coupled IHO has only one noise operator. Thus, the coarse-grained version of the OTOC-LE connection in Eq. (9b) is not reliable. We instead explicitly use the exact form in Eq. (9a), the right-hand side of which reduces to

$$M(t) = \frac{1}{2} + \frac{1}{2}|\langle\psi_2|e^{i(H_2+\delta c_1\hat{x}_2)t} e^{-i(H_2-\delta c_1\hat{x}_2)t}|\psi_2\rangle|^2. \tag{11}$$

Denote $M_1(t) \equiv |\langle\psi|e^{i(H_2+\delta c_1\hat{x}_2)t}e^{-i(H_2-\delta c_1\hat{x}_2)t}|\psi\rangle|^2$. To extract the early exponential growth, consider the quantity $1-\overline{F(t)} \approx 1-M(t) = \frac{1}{2}(1-M_1(t))$. This implies that, in the early growth regime, the averaged OTOC $\overline{F(t)}$ has the same exponential growth rate as $M_1(t)$, but a prefactor half of the latter. Note that the growth of the LE $M(t)$ does not saturate to one. The reason is that the OTOC-LE connection is exact up to second order of the coupling parameter δ. As will be demonstrated in the following, δ^2 plays the role of the prefactor ϵ of the OTOC early growth $\sim\epsilon e^{\lambda t}$, which is precisely reflected in the early growth of the LE. The saturation of the OTOC is induced by higher orders of ϵ.

To see the significance of the coupling strength, we expand $M_1(t)$ to second order of δ using the Baker-Campbell-Hausdorff (BCH) formula, which gives

$$M_1(t) = 1 - \delta^2\frac{4c_1^2c_2^2}{(i\omega_2)^2}\sin^2(i\omega_2 t), \tag{12}$$

where $c_2^2 = \langle\psi_2|x_2^2|\psi_2\rangle$. This describes an exponential Lyapunov growth with rate $2\omega_2$. The second order of the coupling parameter plays the role of the prefactor in the early exponential growth. Derivations for the exact solution of $M_1(t)$ and its second-order BCH expansion are presented in Ref. [55]. Figure 2 depicts the exact solutions of the Haar averaged OTOC $M_1(t)$ as well as the exponential growth extracted from the second-order expansion in Eq. (12). The OTOC-LE connection and the early scrambling are clearly revealed.

Case II: Intermediate decay.—The early exponential growth of the OTOC has been predicted and observed in various platforms (See discussion in Ref. [61] and the references therein). However, in a variety of systems, especially finite-size lattice systems, the scrambling time is typically too small to be reliably visible. Instead, the decay of the OTOC is a pure exponential. To reveal the OTOC-LE relation in such an intermediate decay regime, we study a random matrix model. The model Hamiltonian takes the general form Eq. (6). The noninteracting part of the Hamiltonian are random matrices from the standard Gaussian unitary ensemble (GUE), whose matrix elements have independent real and imaginary parts as Gaussian random numbers with zero mean and unit variance. The small subsystem S_A is chosen as a single qubit. The coupling matrix V_A^k in the decomposition Eq. (6) are chosen as Pauli matrices, i.e., $\{I,\sigma_x,\sigma_y,\sigma_z\}$, while V_B^k on the large subsystem S_B are drawn from the GUE.

The random matrix model has enough complexity to make the OTOC insensitive to the choice of operators. This allows us to numerically simulate the evolution of the OTOC for two random Hermitian operators on the corresponding subsystems. The LE can be computed using the coarse-grained version of the OTOC-LE relation in Eq. (9b). The effective perturbation operators, by Eq. (8),

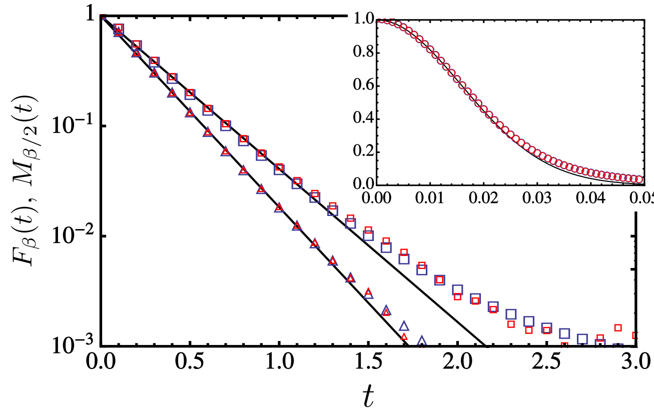

FIG. 3. Numerical simulations of the OTOC and LE for the random matrix model. The Hilbert space dimensions of subsystem S_A and S_B are 2 and 2^9, respectively. Red and blue marks correspond to data of the OTOC and LE, respectively. In the main figure, the coupling parameter is fixed at $\delta = 0.1$, for which the decay is exponential. Triangles and squares correspond to $\beta = 0$ and 0.1, respectively. Inset: Gaussian decay of the OTOC and LE at coupling strength $\delta = 0.5$. The temperature is fixed at infinity. Black lines are best fits to exponential or Gaussian curves.

are the sum of four random matrices from the GUE and, therefore, have matrix elements with variance $4\delta^2$.

It is well known that in the intermediate regime the decay of the LE depends on the strength of the perturbation; i.e., for small perturbations the decay is exponential, while for large perturbations the decay can be Gaussian. Since the relative coupling strength decreases with the system size, exponential decays are typically expected in the thermodynamics limit. However, for small size systems, Gaussian decays might be observed. This explains the Gaussian decay of the OTOC in finite-size systems, e.g., the Sachdev-Ye-Kitaev (SYK) model [17,62,63], for which in the large-N limit the OTOC switches from an early growth to an intermediate exponential decay. As another application of our theory, we present a detailed discussion of the SYK model in Ref. [55].

The numerical simulations for the random matrix model are presented in Fig. 3, where the OTOC and LE are shown to match very well; both exponential and Gaussian decays are revealed.

The bound on chaos.—In the scrambling regime, the early exponential growth rate was conjectured to be universally bounded by the temperature, $\lambda \leq 2\pi/\beta$. This conjecture has been proven under a strong physical assumption that the time-ordered correlators factorize. As a consequence of that assumption, the magnitude of the normalized OTOC is always bounded by unity in the analytic regime on the complex time domain (see Refs. [24,27] for detailed discussions). As another remarkable application of the OTOC-LE connection, we note that the factorization assumption can be removed for the Haar averaged OTOC, which is attributed to the fact that, in the corresponding complex time domain, the LE appears to be averaged over a thermal state with a positive effective temperature. We refer the interested reader to Ref. [55] for a detailed discussion.

Summary.—We have demonstrated the connection between two distinct areas of the dynamical quantum chaos, namely, the emerging field of the out-of-time-order correlators and the relatively more developed field of the Loschmidt echo. This relation not only allows a more general understanding of the universal properties of the OTOC but also provides new insights into both subjects. Two models were used to reveal the OTOC-LE relation in the scrambling regime and the intermediate exponential decay regime. Implications to the bound on the decay rate were also discussed. Future research could generalize the connection to higher-dimensional systems with spatial structures.

This research was supported by the U.S. Department of Energy, Office of Science, Basic Energy Sciences, Materials Sciences and Engineering Division, Condensed Matter Theory Program. W. H. Z. and L. C. were also supported in part by the LDRD program at the Los Alamos National Laboratory. W. H. Z. acknowledges partial support by the Foundational Questions Institute Grant No. FQXi-1821, and Franklin Fetzer Fund, a donor advised fund of the Silicon Valley Community Foundation. L. C. acknowledges support by the DOE through the J. Robert Oppenheimer fellowship. B. Y. and W. H. Z. thank Adolfo del Campo and Nikolai Sinitsyn for helpful discussions.

[1] F. Haake, *Quantum Signatures of Chaos* (Springer-Verlag, Berlin, 2006).

[2] M. Berry, Quantum chaology, not quantum chaos, Phys. Scr. **40**, 335 (1989).

[3] A. Peres, *Quantum Theory: Concepts and Methods*, Fundamental Theories of Physics (Springer, New York, 2002).

[4] W. H. Zurek and J. P. Paz, Decoherence, Chaos, and the Second Law, Phys. Rev. Lett. **72**, 2508 (1994).

[5] W. H. Zurek, Decoherence, chaos, quantum-classical correspondence, and the algorithmic arrow of time, Phys. Scr. **T76**, 186 (1998).

[6] P. R. Levstein, G. Usaj, and H. M. Pastawski, Attenuation of polarization echoes in nuclear magnetic resonance: A study of the emergence of dynamical irreversibility in many-body quantum systems, J. Chem. Phys. **108**, 2718 (1998).

[7] R. A. Jalabert and H. M. Pastawski, Environment-Independent Decoherence Rate in Classically Chaotic Systems, Phys. Rev. Lett. **86**, 2490 (2001).

[8] F. M. Cucchietti, D. A. R. Dalvit, J. P. Paz, and W. H. Zurek, Decoherence and the Loschmidt Echo, Phys. Rev. Lett. **91**, 210403 (2003).

[9] H. Kohler and C. Recher, Fidelity and level correlations in the transition from regularity to chaos, Europhys. Lett. **98**, 10005 (2012).

[10] C. M. Sánchez, P. R. Levstein, L. Buljubasich, H. M. Pastawski, and A. K. Chattah, Quantum dynamics of excitations and decoherence in many-spin systems detected with Loschmidt echoes: Its relation to their spreading through the Hilbert space, Phil. Trans. R. Soc. A **374**, 20150155 (2016).

[11] A. Chenu, I. L. Egusquiza, J. Molina-Vilaplana, and A. del Campo, Quantum work statistics, Loschmidt echo and information scrambling, Sci. Rep. **8**, 12634 (2018).

[12] A Chenu, J. Molina-Vilaplana, and A. del Campo, Work statistics, Loschmidt echo and information scrambling in chaotic quantum systems, Quantum **3**, 127 (2019).

[13] C. M. Sánchez, A. K. Chattah, K. X. Wei, L. Buljubasich, P. Cappellaro, and H. M. Pastawski, Emergent Perturbation Independent Decay of the Loschmidt Echo in a Many-Spin System Studied Through Scaled Dipolar Dynamics, Phys. Rev. Lett. **124**, 030601 (2020).

[14] A. Goussev, R. A. Jalabert, H. M. Pastawski, and D. Wisniacki, Loschmidt echo, Scholarpedia **7**, 11687 (2012).

[15] T. Gorin, T. Prosen, T. H. Seligman, and M. Žnidarič, Dynamics of Loschmidt echoes and fidelity decay, Phys. Rep. **435**, 33 (2006).

[16] A. Larkin and Y. N. Ovchinnikov, Quasiclassical method in the theory of superconductivity, Sov. Phys. JETP **28**, 1200 (1969).

[17] A. Kitaev, A simple model of quantum holography, in *Proceedings of the KITP Program: Entanglement in Strongly-Correlated Quantum Matter, 2015* (Kavli Institute for Theoretical Physics, Santa Barbara, 2015), Vol. 7.

[18] S. H. Shenker and D. Stanford, Black holes and the butterfly effect, J. High Energy Phys. 03 (2014) 067.

[19] S. H. Shenker and D. Stanford, Multiple shocks, J. High Energy Phys. 12 (2014) 046.

[20] D. A. Roberts, D. Stanford, and L. Susskind, Localized shocks, J. High Energy Phys. 03 (2015) 051.

[21] D. A. Roberts and D. Stanford, Diagnosing Chaos Using Four-Point Functions in Two-Dimensional Conformal Field Theory, Phys. Rev. Lett. **115**, 131603 (2015).

[22] M. Blake, Universal Charge Diffusion and the Butterfly Effect in Holographic Theories, Phys. Rev. Lett. **117**, 091601 (2016).

[23] D. A. Roberts and B. Swingle, Lieb-Robinson Bound and the Butterfly Effect in Quantum Field Theories, Phys. Rev. Lett. **117**, 091602 (2016).

[24] J. Maldacena, S. H. Shenker, and D. Stanford, A bound on chaos, J. High Energy Phys. 08 (2016) 106.

[25] W. Fu and S. Sachdev, Numerical study of fermion and boson models with infinite-range random interactions, Phys. Rev. B **94**, 035135 (2016).

[26] P. Hosur, X.-L. Qi, D. A. Roberts, and B. Yoshida, Chaos in quantum channels, J. High Energy Phys. 02 (2016) 004.

[27] N. Tsuji, T. Shitara, and M. Ueda, Bound on the exponential growth rate of out-of-time-ordered correlators, Phys. Rev. E **98**, 012216 (2018).

[28] B. Swingle and D. Chowdhury, Slow scrambling in disordered quantum systems, Phys. Rev. B **95**, 060201(R) (2017).

[29] M. Campisi and J. Goold, Thermodynamics of quantum information scrambling, Phys. Rev. E **95**, 062127 (2017).

[30] X. Chen, T. Zhou, D. A. Huse, and E. Fradkin, Out-of-time-order correlations in many-body localized and thermal phases, Ann. Phys. (Amsterdam) **529**, 1600332 (2017).

[31] E. B. Rozenbaum, S. Ganeshan, and V. Galitski, Lyapunov Exponent and Out-of-Time-Ordered Correlator's Growth Rate in a Chaotic System, Phys. Rev. Lett. **118**, 086801 (2017).

[32] B. Dóra and R. Moessner, Out-of-Time-Ordered Density Correlators in Luttinger Liquids, Phys. Rev. Lett. **119**, 026802 (2017).

[33] K. Hashimoto, K. Murata, and R. Yoshii, Out-of-time-order correlators in quantum mechanics, J. High Energy Phys. 10 (2017) 138.

[34] C.-J. Lin and O. I. Motrunich, Out-of-time-ordered correlators in a quantum Ising chain, Phys. Rev. B **97**, 144304 (2018).

[35] C. J. Lin and O. I. Motrunich, Out-of-time-ordered correlators in short-range and long-range hard-core boson models and in the Luttinger-liquid model, Phys. Rev. B **98**, 134305 (2018).

[36] C. W. von Keyserlingk, T. Rakovszky, F. Pollmann, and S. L. Sondhi, Operator Hydrodynamics, OTOCs, and Entanglement Growth in Systems Without Conservation Laws, Phys. Rev. X **8**, 021013 (2018).

[37] A. Nahum, S. Vijay, and J. Haah, Operator Spreading in Random Unitary Circuits, Phys. Rev. X **8**, 021014 (2018).

[38] V. Khemani, A. Vishwanath, and D. A. Huse, Operator Spreading and the Emergence of Dissipative Hydrodynamics Under Unitary Evolution with Conservation Laws, Phys. Rev. X **8**, 031057 (2018).

[39] H. Gharibyan, M. Hanada, S. H. Shenker, and M. Tezuka, Onset of random matrix behavior in scrambling systems, J. High Energy Phys. 07 (2018) 124.

[40] S. Xu and B. Swingle, Locality, Quantum Fluctuations, and Scrambling, Phys. Rev. X **9**, 031048 (2019).

[41] J. Tuziemski, Out-of-time-ordered correlation functions in open systems: A Feynman-Vernon influence functional approach, Phys. Rev. A **100**, 062106 (2019).

[42] B. Swingle, G. Bentsen, M. Schleier-Smith, and P. Hayden, Measuring the scrambling of quantum information, Phys. Rev. A **94**, 040302(R) (2016).

[43] M. Gärttner, J. G. Bohnet, A. Safavi-Naini, M. L. Wall, J. J. Bollinger, and A. M. Rey, Measuring out-of-time-order correlations and multiple quantum spectra in a trapped-ion quantum magnet, Nat. Phys. **13**, 781 (2017).

[44] J. Li, R. Fan, H. Wang, B. Ye, B. Zeng, H. Zhai, X. Peng, and J. Du, Measuring Out-of-Time-Order Correlators on a Nuclear Magnetic Resonance Quantum Simulator, Phys. Rev. X **7**, 031011 (2017).

[45] K. A. Landsman, C. Figgatt, T. Schuster, N. M. Linke, B. Yoshida, N. Y. Yao, and C. Monroe, Verified quantum information scrambling, Nature (London) **567**, 61 (2019).

[46] J. Kurchan, Quantum bound to chaos and the semiclassical limit, J. Stat. Phys. **171**, 965 (2018).

[47] M. Schmitt, D. Sels, S. Kehrein, and A. Polkovnikov, Semiclassical echo dynamics in the Sachdev-Ye-Kitaev model, Phys. Rev. B **99**, 134301 (2019).

[48] R. Hamazaki, K. Fujimoto, and M. Ueda, Operator noncommutativity and irreversibility in quantum chaos, arXiv:1807.02360.

[49] Ruihua Fan, Pengfei Zhang, Huitao Shen, and Hui Zhai, Out-of-time-order correlation for many-body localization, Sci. Bull. **62**, 707 (2017).

[50] J. Cotler, N. Hunter-Jones, J. Liu, and B. Yoshida, Chaos, complexity, and random matrices, J. High Energy Phys. 11 (2017) 048.

[51] R. de Mello Koch, J.-H. Huang, C.-T. Ma, and H. J. R. Van Zyl, Spectral form factor as an OTOC averaged over the Heisenberg group, Phys. Lett. B **795**, 183 (2019).

[52] C.-T. Ma, Early-time and late-time quantum chaos, arXiv: 1907.04289.

[53] J. S. Cotler, G. Gur-Ari, M. Hanada, J. Polchinski, P. Saad, S. H. Shenker, D. Stanford, A. Streicher, and M. Tezuka, Black holes and random matrices, J. High Energy Phys. 05 (2017) 118.

[54] A. Bhattacharyya, W. Chemissany, S. Shajidul Haque, and B. Yan, Towards the web of quantum chaos diagnostics, arXiv:1909.01894.

[55] See Supplemental Material at http://link.aps.org/supplemental/10.1103/PhysRevLett.124.160603 for derivations of several equations in the main text, and contains one more model study for the SYK model.

[56] W. H. Zurek, Decoherence, einselection, and the quantum origins of the classical, Rev. Mod. Phys. **75**, 715 (2003).

[57] M. Schlosshauer, *Decoherence and the Quantum-To-Classical Transition* (Springer, Berlin, 2007).

[58] A. A. Budini, A. Karina Chattah, and M. O. Cáceres, On the quantum dissipative generator: Weak-coupling approximation and stochastic approach, J. Phys. A **32**, 631 (1999).

[59] A. Romero-Bermúdez, K. Schalm, and V. Scopelliti, Regularization dependence of the OTOC. Which Lyapunov spectrum is the physical one?, J. High EnFergy Phys. 07 (**2019**) 107.

[60] R. Blume-Kohout and W. H. Zurek, Decoherence from a chaotic environment: An upside-down "oscillator" as a model, Phys. Rev. A **68**, 032104 (2003).

[61] S. Xu and B. Swingle, Accessing scrambling using matrix product operators, Nat. Phys. **16**, 199 (2020).

[62] S. Sachdev and J. Ye, Gapless Spin-Fluid Ground State in a Random Quantum Heisenberg Magnet, Phys. Rev. Lett. **70**, 3339 (1993).

[63] J. Maldacena and D. Stanford, Remarks on the Sachdev-Ye-Kitaev model, Phys. Rev. D **94**, 106002 (2016).